Measurement of Flame and Flow Structures of Turbulent Jet Premixed Flame by Simultaneous Triple-Plane PLIF and Dual-Plane Stereoscopic PIV

Masayasu Shimura[1], Ayane Johchi[1], Gyung-Min Choi[2],
Kaoru Iwamoto[3], Mamoru Tanahashi[1], Toshio Miyauchi[1]
[1]Department of Mechanical and Aerospace Engineering, Tokyo Institute of Technology
2-12-1 Ookayama, Meguro-ku, Tokyo 152-8550, Japan
[2]School of Mechanical Engineering, College of Engineering, Pusan National University,
Busan 609-735, Republic of Korea
[3]Faculty of Engineering, Tokyo University of Agriculture and Technology
2-24-16 Naka-cho Koganei-city Tokyo 184-8588, Japan

1   Introduction

Turbulent flame structure has strong interaction with turbulent flow field, which results in the increase of flame area, fluctuation of local heat release rate and so on. Distortion of flame surface in turbulent flow is commonly expressed by the flame curvature and turbulence-induced strain rate at the flame front in the turbulent combustion models, especially in flamelet approach. The recent three-dimensional (3D) DNSs [1][2][3][4][5] have revealed the characteristics of turbulent premixed flames and local flame structures which are hardly expected from theoretical classifications such as turbulent combustion diagrams. Nada et al. [4] has reported that 3D flame structures, which are caused by strong fine scale eddies in turbulence, appear even in laminar flamelet regime of the turbulent combustion diagram supposed by Peters [6]. These characteristics of flame-turbulence interaction should be investigated experimentally.

Laser diagnostics combining planar laser induced fluorescence (PLIF) of molecules or radicals produced in chemical reactions and particle image velocimetry (PIV) have been applied for the investigations of turbulent flame structure [7][8]. However, lots of studies are restricted to the two-dimensional measurements. Since turbulent flames have inherently 3D structure, requirements of 3D measurements have been insisted in previous studies [9][10]. Crossed-plane tomography by Knaus and Gouldin [11] can obtain the 3D flame structure only on the line of intersection. In our previous study [9], dual-plane CH PLIF has been developed and combined with single-plane OH PLIF, which achieves the triple-plane measurement of flame structure, and clarifies the characteristics of 3D flame front and possibility for exact estimation of flame curvature. Due to limitations of single-plane experiments of flow field, strain rate has been evaluated by using velocity gradients only in a measurement plane [12]. However, measurements of three-component velocity and nine-component velocity gradient are necessary to calculate strain rate precisely and to investigate relations between flame structure and turbulence in detail. Paralleled dual-plane tomography and stereoscopic PIV (conditioned PIV) have been utilized for evaluation of the subgrid scalar flux in turbulent premixed
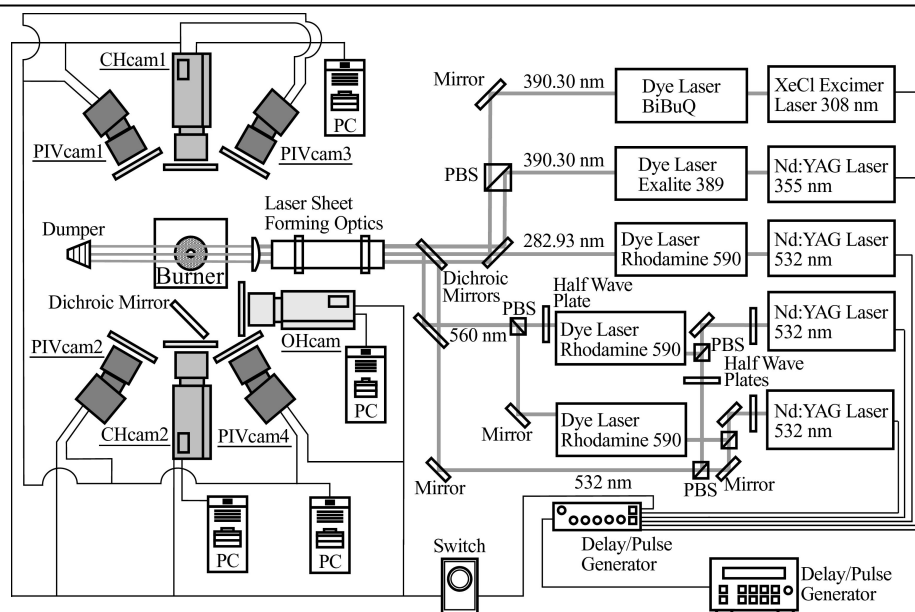
Fig. 1. Schematic diagram of simultaneous triple-plane PLIF and dual-plane stereoscopic PIV.

flames [13], whereas tomography is not always appropriate for identification of flame fronts. In the latest research [14], simultaneous triple-plane PLIF, which consists of dual-plane CH PLIF and single-plane OH PLIF, and dual-plane stereoscopic PIV have been developed and applied to a swirl-stabilized combustor, which shows the necessity of nine-component of velocity gradients to evaluate strain rate in turbulent combustion field.

In this study, the simultaneous triple-plane PLIF and dual-plane stereoscopic PIV are applied to methane-air turbulent jet premixed flame in high Reynolds number, $Re_\lambda = 93.4$, to clarify 3D nature of turbulent premixed flame. In this extended abstract, typical turbulent premixed flame and flow structures are presented. Detailed measurement results enable us to obtain flame front curvature in 3D field and tangential strain rate to flame front.

2   Experimental Method

The schematic of experimental setup for the simultaneous measurement is shown in Fig. 1. The details can be referred in the previous study [14]. For CH PLIF measurement, the $Q_1(7, 5)$ transition of the $B^2\Sigma^--X^2\Pi(0, 0)$ band at 390.30 nm is excited and fluorescence from the A-X(1, 1), (0, 0) and B-X(0, 1) bands between 420 and 440 nm is detected. The dual-plane CH PLIF is comprised of combining two independent CH PLIF systems [9]. Laser beams from each laser system are led to parallel optical pass using the difference of polarization. The parallel beams are expanded into laser sheets by laser sheet forming optics. Fluorescence from excited CH radicals are detected by two intensified CCD cameras (Andor Technology, iStar DH734-25U-03, 1024× 1024 pixels) fitted with 105 mm/f2.8 lens (Nikon, Micro-Nikkor) and optical band-pass filters (Semrock, FF01-434/17-50.8-D, about 92 % transmission) to block flame radiation and scattered light by particles. These cameras are located on the opposite side of the combustor, and optical axes are set to be perpendicular to the laser sheet.

For single-plane OH PLIF, the $Q_1(7)$ transition of the $A^2\Sigma^--X^2\Pi(1, 0)$ band at 282.93 nm is excited and fluorescence from the A-X(1, 1), (0, 0) and B-X(0, 1) bands between 306 and 320 nm is detected. The laser system consists of a Nd:YAG laser (532 nm, 200 mJ/pulse) and a dye laser with Rhodamine 590 dye in ethanol solvent and a second harmonic generator. The laser beam for OH PLIF is led to the axis parallel to the lasers for CH PLIF by a dichroic mirror. The fluorescence from the excited OH radical is reflected by a dichroic mirror and imaged onto the third intensified CCD camera (Princeton Instruments, PI-MAX 51RB-G1, 512× 512 pixels) fitted with UV lens (Nikon, UV-Nikkor, 105
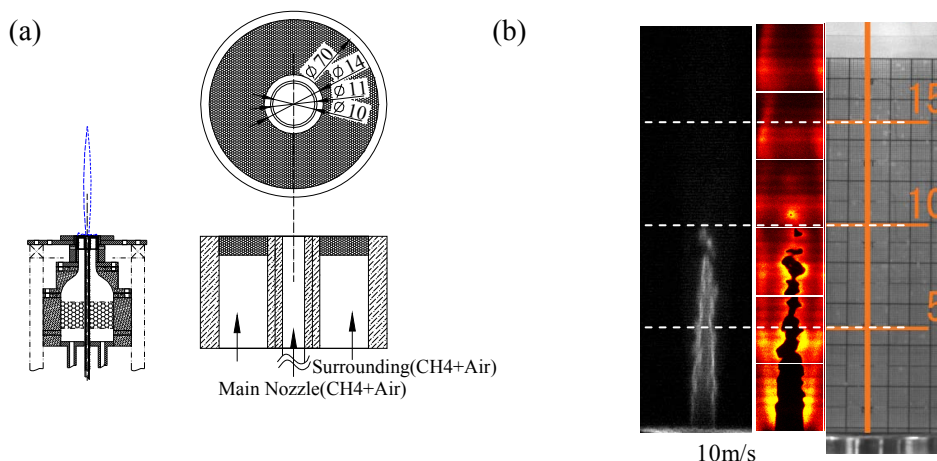
Fig. 2. Schematic of a turbulent jet burner (a) and a CH chemiluminescence image and OH fluorescence image of turbulent jet premixed flame (b).

mm/f4.5) and optical filters (Semrock, FF01-320/40-25, about 80 % transmission). 3D flame structures can be evaluated from triple-plane PLIF of CH and OH radicals by assuming that the edge of OH radical coincides with CH layer.

Dual-plane stereoscopic PIV using nonspherical particles can be accomplished by utilizing the difference of laser wavelength. One plane is illuminated by 532 nm laser and another is done by 560 nm one, which is established by two Nd:YAG lasers (532 nm, 200 mJ/pulse) and two dye lasers with Rhodamine 590 dye in ethanol solvent. The details have been shown in the previous work [14]. The parallel laser sheets expanded by laser sheet forming optics are adjusted to those for dual-plane CH PLIF. Scattered light from particles is imaged onto four double frame CCD cameras (Princeton Instruments, MegaPlus II ES4020, 2048× 2048 pixels) with 200 mm/f4 lens (Nikon, Micro-Nikkor) and a teleconverter (Kenko, Teleplus MC7) which doubles the focal length. The cameras are located at the each side of the ICCD cameras for CH PLIF with about 17.5º to capture stereoscopic particle images, and Scheimpflug condition is applied. Band-pass filters for 532 nm (Semrock, FF01-525/15-25, about 90 % transmission) and 560 nm (Semrock, FF01-560/14-25, about 93 % transmission) are installed to the cameras. As for particles of PIV, to avoid particle flocculation and achieve high particle density, SiO_2 particles with 1 μm diameter, which has small bulk density of about 0.2 g/cm^3, are selected. The high spatial resolution PIV algorithm developed in our previous studies [15] is used to calculate the two-dimensional velocity field from successive particle images obtained by each CCD camera. From two-dimensional velocity fields obtained by each CCD camera, three-component velocity vectors on a two-dimensional plane are calculated by using a geometrical relation. The timing diagram can be seen in the related previous work [9].

3   Experimental Apparatus and Conditions

This simultaneous measurement is applied to methane-air turbulent jet premixed flames shown in Fig. 2. This burner has a main jet nozzle and a surrounding nozzle for flame holding. The inner diameter of the main and the surrounding nozzles are 10 mm and 70 mm, respectively. Figure 2 (b) shows CH chemiluminescence images and OH PLIF images. Note that these images are combined images obtained at different streamwise positions. Table 1 shows experimental conditions and turbulence characteristics of inert flow at the center of jet nozzle. The characteristics were measured by a hotwire constant temperature anemometer with x-probe (Kanomax Japan, Model0250R, tungsten, Φ5 μm) preliminarily. Here, x is distance from the jet exit, Re_D is Reynolds number based on the nozzle diameter (D) and mean axial velocity at the jet exit, Re_λ is Reynolds number based on Taylor microscale (λ) and r.m.s. of velocity fluctuation. (u'_{rms}), u_m is mean velocity, l is integral length scale

Table 1. Experimental conditions

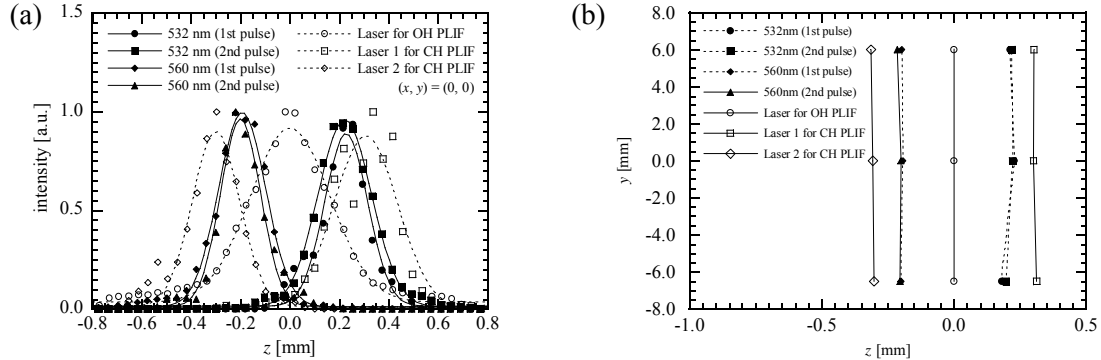| U_0 [m/s]	x/D	Re_D	Re_λ	u_m [m/s]	u'_{rms} [m/s]	l [mm]	λ [mm]	η [μm]	l/δ_F	u'_{rms}/S_L
10	5	6667	93.4	11.40	1.15	6.21	0.998	58.0	150.8	2.88

Fig. 3. Profiles of laser sheets in z direction (a) peak positions of laser sheet profiles on *y-z* plane at *x* = 0 (b) for triple-plane PLIF and dual-plane stereoscopic PIV.

and η is Kolmogorov length. S_L (= 0.399 m/s) is laminar burning velocity and δ_F (= 41.2 μm) is laminar flame thickness which is defined based on kinematic viscosity and S_L. These conditions are classified into the corrugated flamelets in the turbulent combustion diagram by Peters [6]. In this study, simultaneous measurement of dual-plane CH PLIF, single-plane OH PLIF and stereoscopic PIV is conducted for U_0 = 10 m/s. Equivalence ratio ϕ is fixed to 1.0 for the main flame and 0.86 for the surrounding flame. PLIF and PIV were conducted at axial distance of *x/D* = 5. From turbulence and turbulent flame characteristics, the pixel resolutions are set to 29.8 μm/pixel for CH PLIF, 39.0 μm/pixel for OH PLIF and 6.6 μm/pixel for stereoscopic PIV and the measurement regions are about 25 mm × 25 mm for CH and OH PLIF, 13.5 mm × 13.5 mm for stereoscopic PIV. The coordinate system is defined that *x* axis is main flow direction, *y* axis is direction of laser travel and *z* axis is perpendicular to the other axes. This means that the spatial resolution of PIV is determined to be 158.4 μm (≈ 3η) for 24×24 pixels interrogation region and is is same as that of general DNSs of turbulence. This spatial resolution of PIV corresponds to almost same order with that of general DNS of turbulence. Note that the velocity vectors are evaluated with 50 % overlap of the interrogation regions. In this sense, velocity vectors are obtained every 79.2 μm. Time interval of PIV is set to about 3.5 μs.

Figure 3(a) shows the intensity profiles for the laser sheets in the perspective direction at the center of the measurement region. These profiles are measured by a beam profiler (Ophir, FX-50). Peak position of laser for OH PLIF is set to zero. Mean FWHM thicknesses of laser sheets were set to about 210 μm and 260 μm for CH PLIF, 370 μm for OH PLIF and about 220 μm for PIV. Figure 3(b) shows the parallelism of the laser sheets. The distances between laser sheets are 300 μm for triple-plane PLIF and 400 μm for dual-plane stereoscopic PIV within 2.0 mrad through the whole measurement region. These configurations can be changed by regulating the PBSs and dichroic mirrors.

4   Three-Dimensional Turbulent Premixed Flame Structures

Figure 4 shows typical flame structures of methane-air turbulent jet premixed flame obtained by triple-plane PLIF. The visualized domain is 20.0 mm× 20.0 mm. Yellow and black means high and low intensity of fluorescence. Flame structures are heavily fluctuating, and complex flame structures show many differences in three measurement planes even though the separation of each plane is only about 250 μm. In Fig. 4(a), circle A shows the separation of unburnt mixture, and CH radical can be found slightly in the region of the left figure. In the region B, unburnt mixture engulfs burnt gas and CH PLIF images show that two tips of unburnt gas are connecting to each other. In Fig. 4(b), regions C and D also represent engulfment of burnt gas. These engulfment structures cause area and curvature of
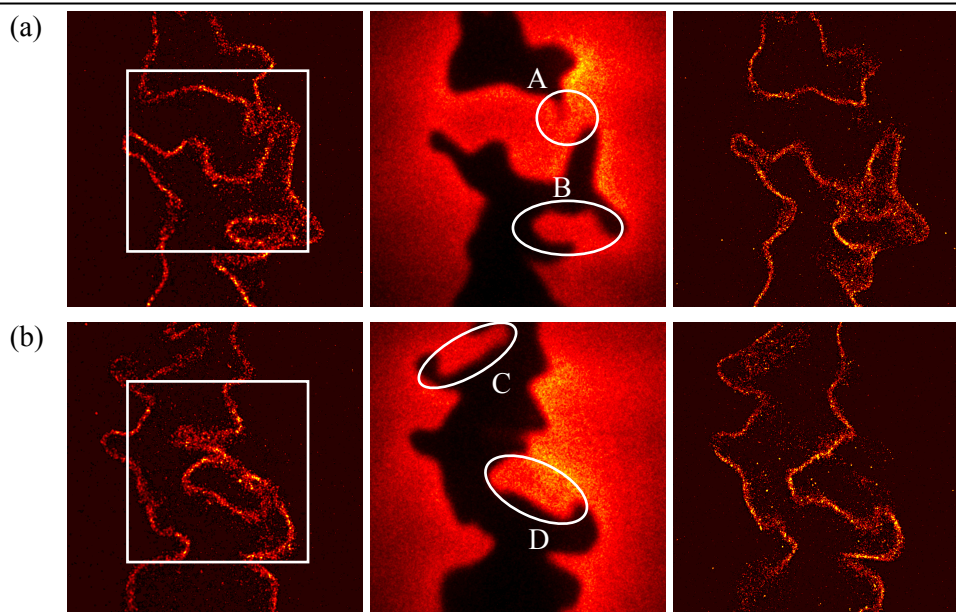
Fig. 4. Examples of fluorescence images (CH PLIF by laser 1, OH PLIF, CH PLIF by laser 2 from the left).
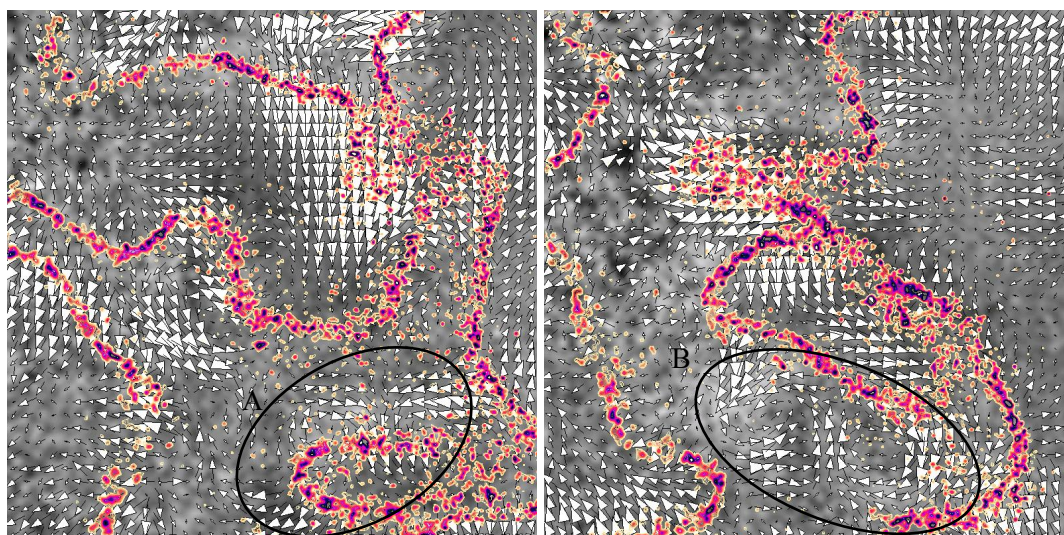

Fig. 5. Examples of CH fluorescence distributions with three components of velocity (vectors: *u* and *v*, grayscale: *w*) obtained by stereoscopic PIV with 532 nm lasers. Visualized region of left and right images corresponds to the white boxes in upper and lower figures in Fig. 4, respectively.

flame front, which might result in increases of heat release rate and total fuel consumption rate. Complicated flame structures are deeply related to flow structure in turbulent jet premixed flame. Figure 5 shows CH fluorescence distributions with three components of velocity obtained by stereoscopic PIV with 532 nm lasers (results obtained by stereoscopic PIV with 560 nm lasers are omitted here). Vectors and grayscale distribution on the back shows *u,v* and *w*, respectively. One-sixteenth of obtained vectors are visualized here. Mean velocity distributions have been obtained from 250 samples and subtracted from instantaneous values. The size of vector represents the magnitude of velocity, and the largest vector corresponds to 2.5 m/s. Region A and B in Fig. 5 show unburnt regions which are close to the engulfment of burnt gas. In both regions, strong vortex structures can be found and might be related to generation of the engulfment. Experimental data of 3D flame structure, three-component of velocity and nine-component of velocity gradients enable us to calculate flame front curvature in three dimensions and strain rate tangential to the flame front. Results of the analyses will

be compared to results obtained from DNS of turbulent premixed flames and presented in 23rd ICDERS.

Acknowledgment

References

[1] Tanahashi M, Fujimura M, Miyauchi T (2000) Coherent fine-scale eddies in turbulent premixed flames. Proc Combust Inst 28:529-535

[2] Jenkins KW, Cant RS (2002) Curvature effects on flames kernels in a turbulent environment. Proc Combust Inst 29:2023-2029

[3] Bell JB, Day MS, Grcar JF (2002) Numerical simulation of premixed turbulent methane combustion. Proc Combust Inst 29:1987-1993

[4] Nada Y, Tanahashi M, Miyauchi T (2004) Effect of turbulence characteristics on local flame structure of H_2-air premixed flames. J Turbulence 5:16

[5] Sankaran R, Hawkes ER, Chen JH, Lu T, Law CK (2007) Structure of a spatially developing turbulent lean methane-air Bunsen flame. Proc Combust Inst 31:1291-1298

[6] Peters N (2000) Turbulent Combustion. London:Cambridge Press

[7] Kalt PAM, Frank JH, Bilger RW (1998) Laser imaging of conditional velocities in premixed propane/air flames by simultaneous OH PLIF and PIV. Proc Combust Inst 27:751-758

[8] Tanahashi M, Murakami S, Choi GM, Fukuchi Y, Miyauchi T (2005) Simultaneous CH-OH PLIF and stereoscopic PIV measurements of turbulent premixed flames. Proc Combust Inst 30:1665-1672

[9] Ueda T, Shimura M, Tanahashi M, Miyauchi T (2009) Measurement of three-dimensional flame structure by combined laser diagnostics. J Mech Sci Technol 23 (7):1813-1820

[10] Chen YC (2009) Measurements of three-dimensional mean flame surface area ratio in turbulent premixed Bunsen flames. Proc Combust Inst 32:1771-1777

[11] Knaus DA, Gouldin FC (2000) Measurements of flamelet orientations in premixed flames with positive and negative Markstein numbers. Proc Combust Inst 28:367-373

[12] Donbar JM, Driscoll JF, Carter CD (2001) Strain rates measured along the wrinkled flame contour within turbulent non-premixed jet flames. Combust Flame 125:1239-1257

[13] Pfadler S, Kerl J, Beyrau F, Leipertz A, Sadiki A, Scheuerlein J, Dinkelacker F (2009) Direct evaluation of the subgrid scale scalar flux in turbulent premixed flames with conditioned dual-plane stereo PIV. Proc Combust Inst 32:1723-1730

[14] Shimura M, Ueda T, Choi GM, Tanahashi M, Miyauchi T (2011) Simultaneous dual-plane CH PLIF, single-plane OH PLIF and dual-plane stereoscopic PIV measuremetns in methane-air turbulent premixed flame, Proc Combust Inst 33:775-782

[15] Tanahashi M, Hirayama T, Taka S, Miyauchi T (2008b) Measurement of fine scale structure in turbulence by time-resolved dual-plane stereoscopic PIV. Int J Heat Fluid Flow 29:792-802